High Doses of Radiation Cause Cochlear Immunological Stress and Sensorineural Hearing Loss

Mengwen Shi , Huiwen Yang , Ye Wang , Chengcai Lai , Jintao Yu * , Yu Sun *

Posted Date: 22 January 2024

doi: 10.20944/preprints202401.1522.v1

Keywords: Radiation; Sensorineural hearing loss; Macrophage; Cochlear Inflammation

Article

High Doses of Radiation Cause Cochlear Immunological Stress and Sensorineural Hearing Loss

Mengwen Shi [1,†], Huiwen Yang [1,†], Ye Wang [2,†], Chengcai Lai [3,*], Jintao Yu [1,*] and Yu Sun [1,*]

[1] Department of Otorhinolaryngology, Union Hospital, Tongji Medical College, Huazhong University of Science and Technology, Wuhan, 430022, China.
[2] Cancer center, Union Hospital, Tongji Medical College, Huazhong University of Science and Technology, Wuhan 430022, Hubei, China.
[3] Department of Pharmaceutical Sciences, Beijing Institute of Radiation Medicine, Beijing 100850, China.
* Correspondence: sunyu@hust.edu.cn (Y.S.); jintaoyu@hust.edu.cn (J.T.); asa2057516@163.com (C.L.).
† These authors contribute equally to this work.

Abstract: Radiotherapy is a crucial treatment for head and neck malignancies, but it usually leads to sensorineural hearing loss (SNHL). Changes in the immune microenvironment and sensorial neuroepithelium of the inner ear after radiation exposure remain poorly understood. This study investigated cochlear morphology and macrophages in the inner ear after high-dose irradiation. The heads of 8-week-old Cx3cr1$^{GFP/+}$ heterozygous male mice were irradiated with 30Gy X-rays and biological samples were taken on the 1st, 7th, and 10th days after irradiation. Auditory brainstem responses were used to assess auditory function in mice. The changes of basal membrane hair cells, spiral ganglion (SGN), and inner ear macrophages were observed using hematoxylin-eosin (HE) staining and immunofluorescence staining. The expression of inflammatory mediators in the inner ear was detected by reverse transcription-polymerase chain reaction (RT-PCR) in cochlear tissue. As a result, there was no significant hair cell loss after high doses of radiation, but the mice developed full-frequency hearing loss on day 10 when HE staining revealed SGN atrophy and immunofluorescence revealed decreased neurofilament expression. The number of macrophages in the inner ear decreased over time. RT-PCR showed that cochlear inflammatory factors and chemokines were briefly up-regulated on the first day after irradiation and then decreased over time. In summary, high-dose irradiation causes acute SNHL that does not involve hair cell loss and may be associated with SGN changes. Radiation-induced SNHL is accompanied by a reduction in cochlear macrophages and changes in the immune microenvironment, but the relationship between the two has yet to be explored.

Keywords: radiation; sensorineural hearing loss; macrophage; cochlear inflammation

1. Introduction

Radiotherapy is an important treatment for head and neck tumors. However, during the treatment, the temporal bone and its accessory structures are often difficult to avoid exposure to ionizing radiation, resulting in damage to auditory pathways [1,2] including conductive hearing loss (such as otitis media, ossicular chain necrosis, etc.) and sensorineural hearing loss, which is manifested as delayed, progressive and irreversible hearing loss, often with high-frequency hearing loss as the first [3]. In an open-label, phase 2, randomized trial of oropharyngeal squamous cell carcinoma, radiation-induced sensorineural hearing loss (RISNHL) occurred in 38% of patients after radiotherapy [4]. Research on children who suffered head-and-neck tumors confirms that the onset of high-frequency hearing loss will be accelerated by platinum-based chemotherapy if mean cochlea radiation doses are > 20 Gy. Patients develop a rapid onset of lower-frequency hearing loss after early high-dose radiation (> 30 Gy) exposure regardless of platinum exposure, and this RISNHL continues to increase in incidence over time [5]. Even though the timing and degree of ototoxicity after radiotherapy varies clinically, and the correlation between ototoxicity and ionizing radiation dose remains unclear, it is of particular interest to study the pathogenesis of RISNHL.

 doi:10.20944/preprints202401.1522.v1

Changes in inner ear morphology and auditory pathways after ionizing radiation are widely recognized to be related to tissue absorption dose and exposure time. Currently, the oxidative stress-apoptosis theory is the prevailing view to explain the dysfunction and death of auditory-related cells in the inner ear and RISNHL. Ionizing radiation directly causes DNA damage, including double-strand breaks, and produces large amounts of oxygen radicals. The unusually high concentrations of reactive oxygen species (ROS) within tissues result in metabolic dysregulation and structural/functional alterations [6]. Meanwhile, ionizing radiation disrupts vascular permeability [7] and causes dysfunction of cochlear lymphatic circulation [8]. Temporary dysfunction of cochlear microcirculation may indirectly affect sensory epithelium function and survival. In the cochlear radiation model, disruption of the stria vascularis (SV) and loss of the outer hair cells (OHCs) in mice are verified to be attributed to ROS-related increases in the 4-HNE level and DNA damage-related increases in the level of poly (ADP-ribose) polymerase-1. The modulation of ROS by antioxidants in C57BL/6 mice reduced radiation-induced inner ear damage and hearing loss [9,10]. It is also reported that the cochlear ribbon synapse is very sensitive to ionizing radiation, and this pathological change can occur in the acute phase after irradiation [11]. Radiation-induced tissue cell death is confirmed with the generation of ROS and the consequent activation of caspase, inflammation, apoptosis [12], and/or necrosis [13]. The biological functions of the body's immune system are diverse. In the past, the inner ear was wrongly thought to be an immunologically exempt organ because of the blood-labyrinth barrier in the inner ear. However, in recent years, it has been found that the activation and aggregation of inner ear macrophages are closely related to hair cell survival and hearing function in noise-induced deafness [14] and gjb2 hereditary deafness models [15]. They demonstrated that the death of cochlear hair cells or neurons due to external stimulation is often accompanied by macrophage aggregation and local inflammation. Macrophages can remove necrotic cells and activate an immune inflammatory response in the inner ear, which affects the function of inner ear hair cells. However, evidence has shown that macrophage overactivation and macrophage-associated immune inflammatory response may be a bidirectional process [16], and the specific contribution of this response to auditory cell function is not well defined. More importantly, the role of post-radiation changes in cochlear immune cells and inflammatory mediators remains unclear, and in particular, the role of cochlear macrophage-related immune inflammatory responses in radiation-induced ear injury remains to be elucidated.

In this study, we first model sensorineural hearing loss induced by high doses of radiation. We then looked at the effects of ionizing radiation on auditory-related cells and macrophages in the inner ear of mice and detected changes in circulation and cochlear inflammatory mediators in mouse immune cells in the short-term after high-dose radiation to elucidate the pathogenesis of RISNHL.

2. Materials and Methods

2.1. Animals

In this study, 8-week-old male Cx3cr1$^{GFP/+}$ heterozygous mice were bred in-house on a CBA/j background. The GFP gene replaces one allele of CX3CR1, a fractalkine receptor. Cx3cr1 is expressed in macrophages, monocytes, microglia, NK cells, and related cells [14]. As a result, Cx3cr1$^{GFP/+}$ mice can express GFP in all macrophages, facilitating the tracking of the number and location of macrophages in the interior. Auditory brainstem response (ABR) tests were performed on all mice before the experiment to ensure they have quite a good hearing function. All the mice were bred in the SPF Animal Room of the Laboratory Animal Center of Tongji Medical College, Huazhong University of Science and Technology. The operator holds the Laboratory Animal Professional Technical Examination certificate.

2.2. Radiation exposure

Mice were anesthetized by Zoletil 50(30 mg/kg, Virbac, Fronce) and Xylazine (10 mg/kg, LGM Pharma, America) through intraperitoneal injection. The irradiation field was adjusted to 8 cm ×40 cm covering the cranial of several mice. The source axis distance to the shaft was 100 cm and the

 doi:10.20944/preprints202401.1522.v1

thickness of the lead block was 10 cm [17]. Mice were irradiated with a single dose of 30 Gy by 6-MV X-rays (600 MU min−1, Trilogy System Linear Accelerator, Varian Medical Systems) [17].

2.3. Auditory brainstem response

After being deeply anesthetized, the mice were placed in a thermostatic blanket to maintain body temperature during the measurement. There were three electrode pins to be placed, the reference electrode was inserted under the skin of the mastoid of the test ear (reversed electrode), the recording electrode was inserted under the skin of the median cranial top of the mouse (simultaneous electrode), and the common electrode was inserted under the skin of the mastoid of the opposite ear (grounded). The computer's TDT system is turned on to generate the stimulus sound, which is amplified by the device and transmitted to a speaker and then to the ear, where the evoked potential is transmitted to a signal processor in the computer for superposition processing. The stimuli were short pure tones at 4 kHz, 8 kHz, 12 kHz, 16 kHz, 20 kHz, 24 kHz, 28 kHz, and 32 kHz with a repetition rate of 10 per second, a scan time of 10 ms, and a superposition of 512 times. The sound intensity of the test starts at 90dB SPL and gradually decreases by 5dB SPL after approaching the threshold value, which is represented by the sound intensity of the ABR II wave in the brainstem potential wave group that can be recognized by the naked eye [18].

2.4. Blood sample and cochlear acquisition

Under anesthesia following the ABR test, the eyeballs of the mice were quickly removed and we obtained blood from the retroorbital venous plexus. The blood is collected into a glass tube pre-filled with anticoagulant until the bleeding stops. The mice were then killed by cervical dislocations, with the cochlea carefully detached from the temporal bone and placed in pre-cooled, fresh 4% paraformaldehyde. The circular and oval windows of the cochlea were opened under a microscope, and the cochlea was rinsed with an infusion of paraformaldehyde with a needle to make the cochlea white. The cochlea was placed in 4% paraformaldehyde in a refrigerator at 4℃ overnight.

2.5. Hematoxylin-eosin (HE) staining

The cochlear section was immersed in PBS solution for 10 min for OCT removal, 3 min for hematoxylin, and washed with tap water for 30 seconds. Dip in 1% ethanol for 2s, dye in eosin for 4min, dip in 95% ethanol for 2min, dip in anhydrous ethanol for 2min, clear with xylene for 10min, then seal with neutral glue.

2.6. Immunofluorescence staining

After the fixed cochlea was decalcified in 10% EDTA solution for 24 hours, for frozen sections, the cochlea was dehydrated with 10%, 20%, and 30% sucrose solutions for 1 hour, respectively, and embedded in optimal cutting temperature compound (OCT) overnight at 4℃. A section of the medial axis of the cochlea with a thickness of 10 mm was removed for subsequent experiments. For basilar membrane placement, each cochlea was carefully dissected in 0.01 M of frozen PBS. Cochlear sections or basement membrane products were incubated in a blocking solution (10% Donkey serum plus 0.1% Triton X-100) at room temperature for 1 hour. The samples were then incubated with rabbit anti-GFP polyclonal antibody (1:200 dilution, M048-3, MBL, Beijing, China) or anti-Neurofilament Heavy Chain antibody (1:500 dilution, AB5539, Sigma-Aldrich, America) at 4℃ overnight. The samples were washed 3 times in 0.01 M PBS containing 0.1% Tween-20, and then stained with Alexa Fluor 647 Donkey Anti-Rabbit IgG (1:200 dilution, ANT032, Antgene, China) or Alexa Fluor 488 Donkey Anti-Chicken IgY (1:200 dilution, A78948, Thermo Fisher Scientific, America) for 2 hours. DAPI (C1005, Beyotime Biotechnology) and phalloidin (0.05 mg/ml, P5282, Sigma-Aldrich) were used for nuclear and F-actin staining. Images were obtained using laser scanning confocal microscopy (Nikon, Tokyo, Japan). Macrophages were visualized using GFP immunostaining.

2.7. Cell count

 doi:10.20944/preprints202401.1522.v1

The basal membrane was scanned and 3D reconstructed under a 10× mirror. The ImageJ software was used to take 1.5 mm lengths at the top, transition, and bottom, respectively. The region between the inner hair cells and the third exclusive hair cell is the sensory-sensitive neuroepithelial region.

2.8. RNA preparation and real-time quantitative polymerase chain reaction

RT-qPCR detected transcriptional expression levels of the following genes: TNF-α, IL-1β, IL-6, CCL2, CCL3, and CCL4. After killing the animal, the connective tissue around the cochlea was carefully removed from the ice. One cochlea was used as a sample and six biological replications were performed for each experimental condition. Total RNA was extracted from collected tissues using FastPure Cell/Tissue Total RNA Isolation Kit V2 (Vazyme. Nanjing, China). Reverse transcription was performed using HiScript III 1st Strand cDNA Synthesis Kit (+gDNA wiper) (Vazyme. Nanjing, China). RT-qPCR was performed on the Roche LightCycler 480 instrument using the SYBR green PCR technique. Each group's relative gene expression data were analyzed by standard method 2-△ct. RT-qPCR uses the following primers:

GAPDH Forward GCCAAGTATGATGACATCAAGAAGG
GAPDH Reverse GCTGTAGCCGTATTCATTGTCATAC
IL-1β Forward GAAATGCCACCTTTTGACAGTG
IL-1β Reverse TGGATGCTCTCATCAGGACAG
IL-6 Forward AATTTCCTCTGGTCTTCTGGAGTAC
IL-6 Reverse GACTCCAGCTTATCTGTTAGGAGAG
TNFα Forward CAGGCGGTGCCTATGTCTC
TNFα Reverse CGATCACCCCGAAGTTCAGTAG
CCL3 Forward GCAACCAAGTCTTCTCAGCG
CCL3 ReverseTCTCTTAGTCAGGAAAATGACACC
CCL4 Forward TGTGCAAACCTAACCCCGAG
CCL4 ReverseGGGTCAGAGCCCATTGGTG
CCL2 Forward TAAAAACCTGGATCGGAACCAAA
CCL2 ReverseGCATTAGCTTCAGATTTACGGGT

2.9. Statistical analysis

Statistics were performed using GraphPad Prism 8.0 (GraphPad Software Inc., La Jolla, CA, USA) and IBM SPSS Statistics 21.0 (SPSS Inc., Chicago, IL, USA). All values in the figures were presented as mean ± standard deviation (SD). For three or more groups, we first performed an ANOVA analysis. For a P value < 0.05, we then used t-tests to compare pairs of subgroups. We compared the data between groups using an unpaired, two-tailed Student's t-test. $P < 0.05$ is considered statistically significant.

3. Results

3.1. Changes in peripheral immune cells in mice after a single localized high dose of ionizing radiation

The body weight of 8-week-old mice with a body weight of 18g-22g was measured at a fixed time every day after a single 30Gy whole-head X-ray irradiation (Figure 1a,b). Day 1st, day 7th, and day 10th after irradiation were selected as the observation time, and the body weight of the mice gradually decreased with time (Figure 1c). Compared with before irradiation, there was no significant difference in weight loss on day 1 after irradiation (21.07±1.6g vs. 19.95±2.98g, p=0.1575, n=6). Compared with before irradiation, the weight of mice decreased significantly on day 7 (21.17±1.73g vs. 15.7±1.15g, p=0.0003, n=6) and day 10 (23.88±2.15g vs. 15.88±0.73g, p=0.0002, n=6) after irradiation. The difference was statistically significant. By the seventh day after irradiation, the mice had lost about 25 percent of their body weight, which showed up as slightly coarser hair, followed by a sharp downward shift in the overall body state. By day 10, some of the mice had lost more than 30 percent of their body weight and showed signs of multiple organ failure, such as navicular abscesses, coarse

 doi:10.20944/preprints202401.1522.v1

hair, sunken eyeballs, and erratic gait. The severity of systemic adverse reactions may be related to animal susceptibility to radiation and individual differences [19].

The total number of white blood cells, lymphocytes, and intermediate cells (Figure 1d–f) in the venous blood of the mice was very sensitive to ionizing radiation and decreased significantly on the first day after exposure. Intermediate cells are a group of cells classified by three groups of leukocytes and include the sum of eosinophils, basophils, and monocytes [20]. The number of cells decreases as the observation time lengthens. The WBC count of control group, P1d, P7d and P10d was 2.62±0.48 10^9/L, 1.83±0.59 10^9/L, 1.66±0.86 10^9/L, 1.14±0.56 10^9/L, respectively. The WBC was reduced in all irradiated groups compared to the control group. The difference was statistically significant (F=6.386, p=0.0025, n=7). The absolute values of lymphocytes in the control group, P1d, P7d, and P10d were 4.1±0.83 10^9/L, 1.16±0.2 10^9/L, 0.7±0.19 10^9/L, 0.46±0.14 10^9/L, respectively. All irradiation groups were significantly lower than the control group (F=4.176, p=0.0143, n=7), and P7d and P10d were also significantly lower than P1d (F=86.36, p <0.0001, n=6). The neutrophil counts of P1d, P7d and P10d were 0.09±0.05 10^9/L, 0.06±0.03 10^9/L, 0.03±0.02 10^9/L, respectively, which were significantly decreased compared with 0.15±0.04 in the control group (F=11.83, p <0.0001, p < 0.05. n=7). Combined, these findings suggest that high doses of irradiation trigger a systemic response. Immune cells in the peripheral blood of the mice were very sensitive to the radiation and were inhibited for a short time.

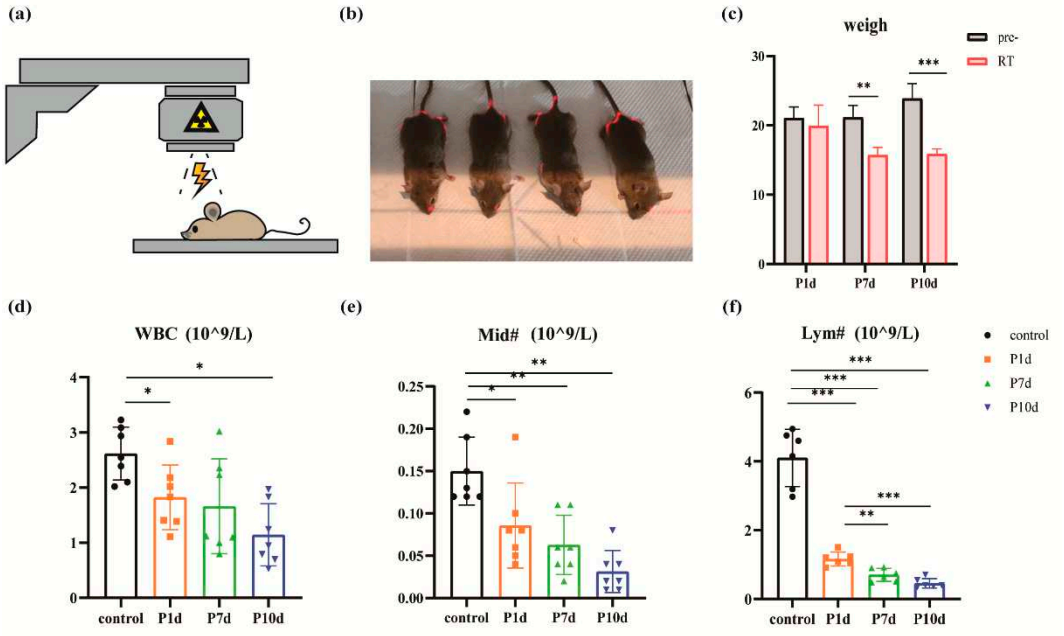

Figure 1. Radiation model and peripheral immune cell changes in mice. (**a**)-(**b**) The exposure pattern of the mouse and the yellow light region is that of the irradiated region. (**c**) Significant weight loss after exposure to ionizing radiation (** p < 0.01) (*** p < 0.001). (**d**)-(**f**) Changes in white blood cell (WBC) count, the absolute value of lymphocytes (Lym#), and the absolute value of intermediate cell (Mid#) in peripheral blood of mice on day 1st, day 7th, and day 10th after radiation exposure. (n = 6 in each group).

3.2. Changes in inner ear macrophages and inflammatory mediators in mice after a high dose of irradiation

Cochlear macrophages and nuclei were labeled with GFP (green) and DAPI (blue) immunofluorescence, respectively, and the number of cochlear macrophages decreased after noise exposure under confocal laser microscopy (Figure 2a,b). In the parietal basement membrane region, compared with the control group (14.75±1.96), the number of macrophages in P1d group (8.08±2.64), P7d group (4.75±1.54) and P10d group (3.92±1.93) were significantly decreased, with statistical significance (F=68.71, p<0.0001, n=12). The number of macrophages in the P7d and P10d groups was significantly lower than that in the P1d group, and the difference was statistically significant (* p <

 doi:10.20944/preprints202401.1522.v1

0.05, ** p < 0.01, *** p < 0.001, **** p < 0.001). There was no significant difference in the number of macrophages between P7d group and P10d group (Figure 2c); in basal membrane transfer (Figure 2d), the number of macrophages in the control group, P1d group, P7d group, and P10d group was 17.08±4.72, 9.67±2.77, 5.25±1.54 and 4.08±1.62, respectively. The number of macrophages decreased significantly in the three groups exposed to radiation, with statistical significance ($F=47.58$, $p<0.0001$, $n=12$). The number of macrophages in P7d and P10d groups was significantly lower than that in P1d group, with statistical significance (* p < 0.05, ** p < 0.01, *** p < 0.001, **** p < 0.001), but there was no statistical difference between P7d and P10d groups. Basal membrane rotation (Figure 2e) was compared between the control group (9.83±3.35), P1d group (5.67±1.23), P7d group (3.75±0.87) and P10d group (2.25±1.36). The differences were statistically significant (* p < 0.05, ** p < 0.01, *** p < 0.001, **** p < 0.001).

The expression of inflammatory factors IL-1β, IL-6, TNF-α, and chemokines CCL2, CCL3, and CCL4 in mouse cochlear were quantitatively evaluated by RT-PCR. The results showed that all the above inflammatory mediators significantly increased in P1d, and then showed a downward trend with the observation time (Figure 3).

Together, this demonstrates that macrophages in the basilar membrane region of the cochlea are sensitive to radiation and decrease significantly with time after radiation exposure. At the same time, inflammatory mediators in the cochlea increased rapidly after radiation and then decreased.

 doi:10.20944/preprints202401.1522.v1

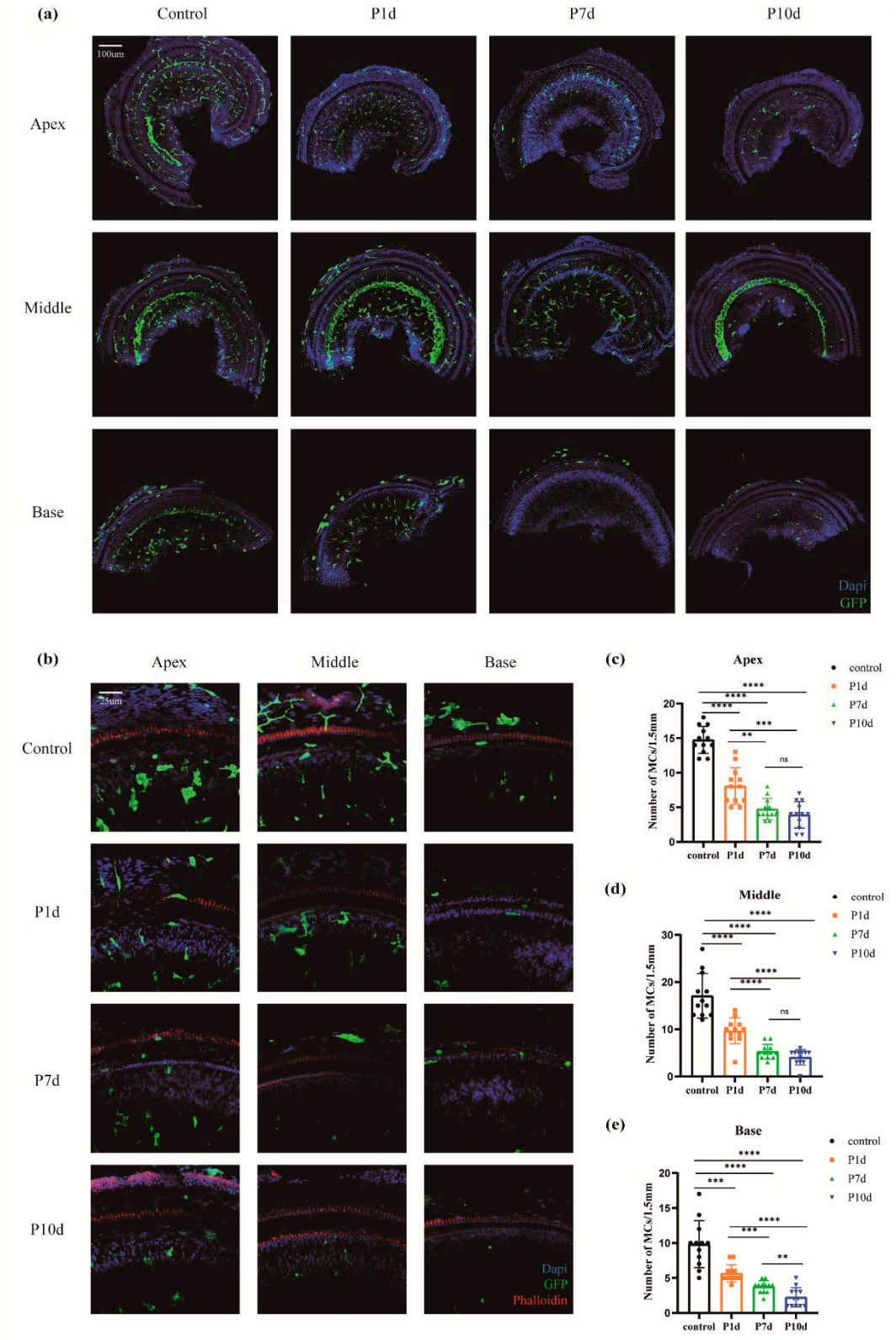

Figure 2. Macrophages in the basement membrane region gradually decline after exposure to ionizing radiation. (**a**) Macrophages in the whole segment of the cochlear membranous labyrinth of mice at day 1st, day 7th, and day 10th after irradiation under a 10-fold laser confocal microscope (blue DAPI, green GFP, scale 200um). (**b**) Representative pictures of macrophages at the top, middle, and bottom of the cochlear membrane labyrinth of mice on day 1st, day 7th, and day 10th after irradiation (40×, scale 50um). (**c**)-(e) Macrophage counts in the parietal, middle, and basal basement membrane regions of the cochlear membrane of mice at day 1st, day 7th, and day 10th after irradiation (n = 6 in each group).

 doi:10.20944/preprints202401.1522.v1

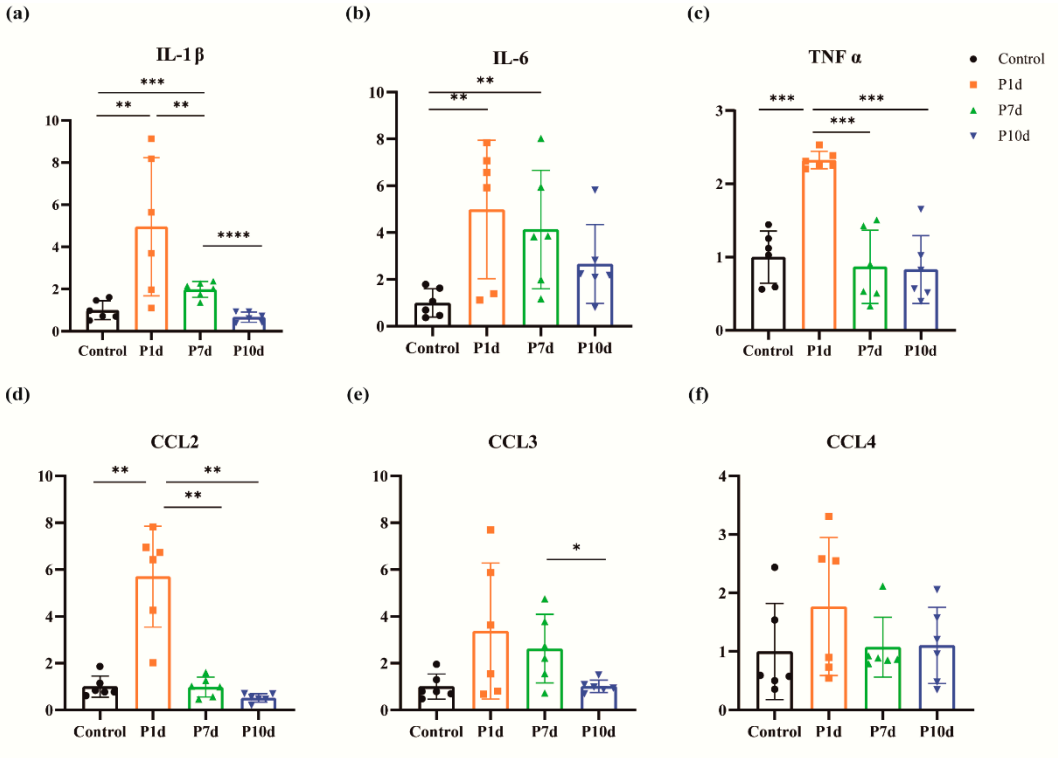

Figure 3. Changes in inflammatory mediators in the inner ear following exposure to ionizing radiation. (**a**) Changes of IL-1β in the cochlea of mice in the control group and on day 1st, day 7th, and day 10th after irradiation. (**b**) Changes in IL-6 in the cochlea of mice in the control group and at day 1st, day 7th, and day 10th after irradiation. (**c**) Changes of TNF*α* in the cochlea of mice in the control group and on day 1st, day 7th, and day 10th after irradiation. (**d**) Changes in CCL2 in the cochlea of mice in the control group and on day 1st, day 7th, and day 10th after irradiation. (**e**) Changes in cochlear CCL3 at day 1st, day 7th, and day 10th after irradiation in the control and study groups. (**f**) Changes in cochlear CCL4 at day 1st, day 7th, and day 10th after irradiation in the control group and in the study groups. (n = 6 in each group).

3.3. Mice exposed to high doses of irradiation showed impaired hearing function with no hair cell loss in the short term

The ABR hearing test was used to assess hearing in mice. Compared to before exposure, The click threshold of mice (Figure 4a) was observed in P1d (15.83± 2.04dB vs. 13.33± 2.58dB, p=0.0756, n=6), P7d (15± 5.48dB vs. 17.5±4.18dB, p=0.2956, n=6) There was no significant threshold shift, and the threshold increased in the P10d group (15.83± 2.04dB vs. 47.5± 7.58dB, p=0.0001, n=6). Statistical analysis was performed on click ABR 1 wave latency (Figure 4b) and amplitude (Figure 4c) of mice. No statistically significant difference was found between P1d and P7d, and the delay in the P10d group was longer than before irradiation, but the difference was not statistically significant. The amplitude decreased (9.86±0.97 uV vs. 3.42±2.53 uV, p=0.0009, n=6). At 8, 12, 16, 20, 24, 28, and 32 kHz, there was no significant threshold shift in ABR hearing on P1d and P7d, while the threshold in the P10d group increased significantly (Figure 4d). The incubation period and amplitude of ABR-I wave at 8, 12, 16, 20, 24, 28, and 32 kHz in each group were statistically analyzed, and it was found that compared with before irradiation, the incubation period of ABR-I wave in P1d group and P7d group did not show significant changes at each frequency, while the incubation period of ABR-I wave in P10d group was prolonged and the amplitude decreased, with statistically significant differences (Figure 4e–j).

The hair cells cilia and nucleus were labeled by phalloidin(red) and DAPI (blue) under confocal laser microscopy. The entire segment of the basement membrane was observed under a 10× objective

 doi:10.20944/preprints202401.1522.v1

lens, and no significant hair cell loss was observed in the irradiated group (Figure 5a,b); there was no decrease in outer hair cell survival compared to the control group (Figure 5c–e).

Collectively, these data reveal that the acute phase of high-dose radiation resulted in full-frequency hearing loss in mice without hair cell loss.

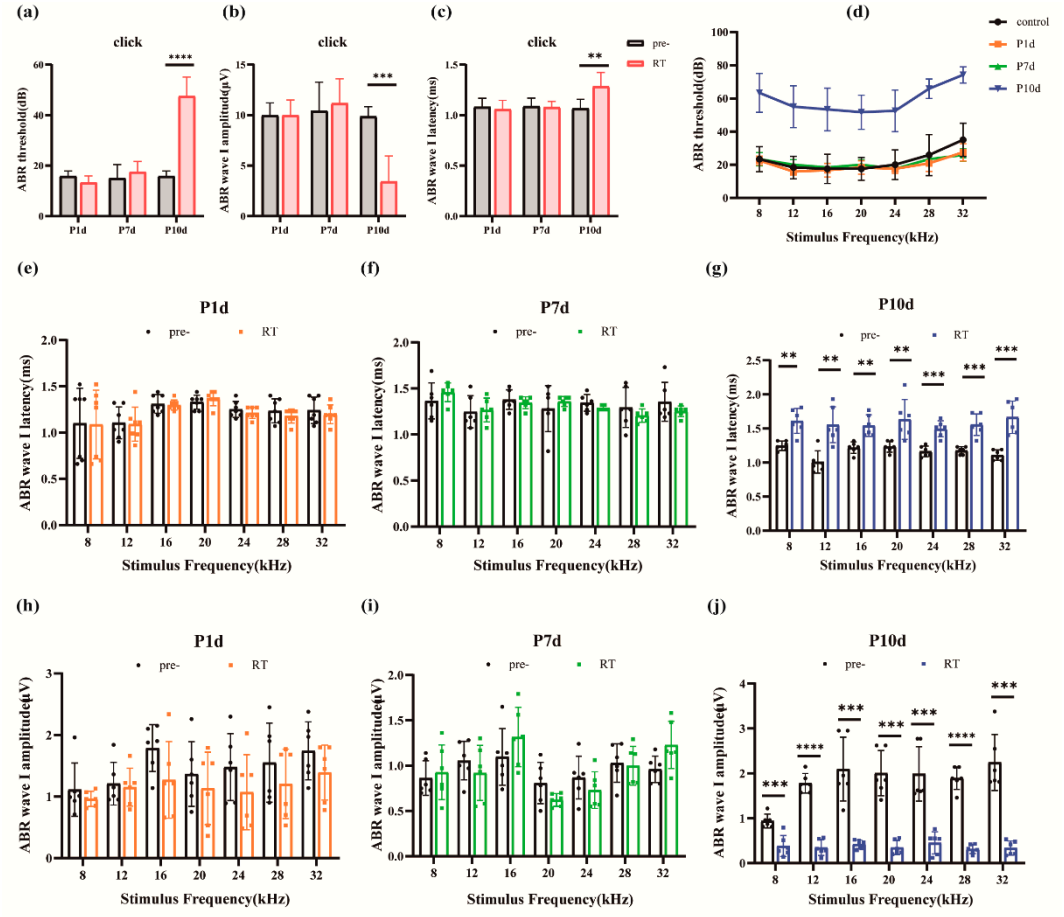

Figure 4. Effects of ionizing radiation exposure on ABR hearing in mice. (**a**)-(**c**) Changes in click threshold, I-wave amplitude, and I-wave delay for mice on day 1st, day 7th, and day 10th after irradiation. (**d**) Variations of the ABR threshold at different frequencies in mice on days 1, 7, and 10 after irradiation. (e)-(**g**). Changes in the latency of the I-wave at different frequencies on day 1st, day 7th, and day 10th after irradiation in mice. (**h**)-(**j**) I-wave amplitude variations at different frequencies on day 1st, day 7th, and day 10th after irradiation in mice. (n = 6 in each group).

 doi:10.20944/preprints202401.1522.v1

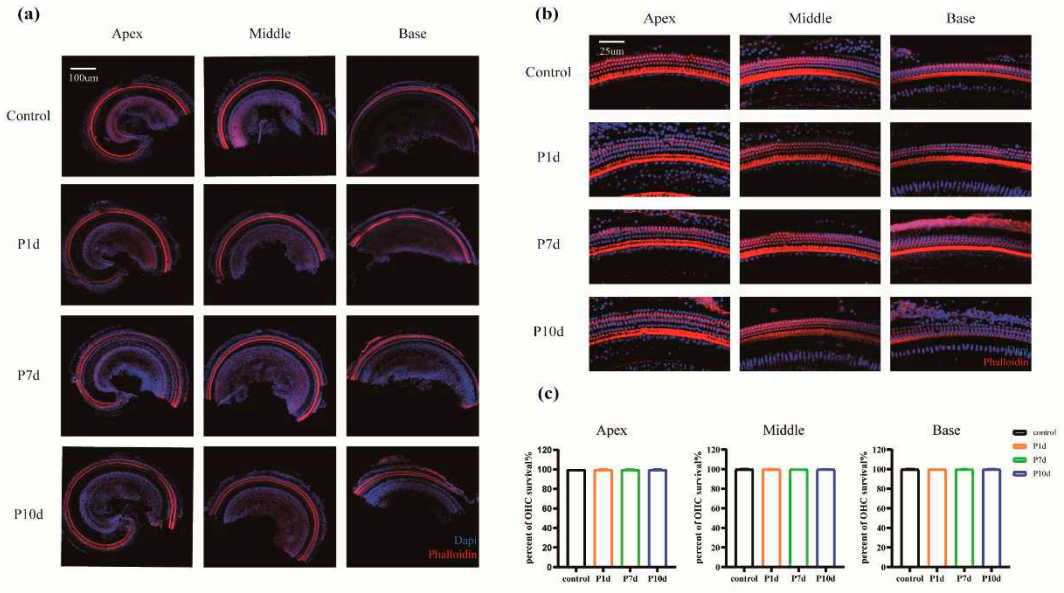

Figure 5. Ear hair cells were not damaged during the acute period of ionizing radiation. (**a**) Hair cells in all segments of the cochlear membranous labyrinth of mice at day 1st, day 7th, and day 10th after irradiation under a 10-fold laser confocal microscope (blue DAPI, red phalloidin, scale 200um). (**b**) Representative pictures of the top, middle, and bottom hair cells of the cochlear membrane of mice on day 1st, day 7th, and day 10th after irradiation (40×, scale 50um). (**c**)-(**e**) The survival rate of outer hair cells of the apex, middle, and base of the cochlear membrane of mice at day 1st, day 7th, and day 10th after irradiation (n = 6 in each group).

3.4. High-dose radiation-induced morphological changes in SGN

HE staining of cochlear sections showed that SGN cells of the inner ear of mice showed morphological changes on the tenth day after irradiation (Figure 6). Compared to the control group, cells in the SGN and medial axis regions of the cochlea in the P10d group were more deeply stained, and the interstitial tissue was reduced, but the density of the cell distribution did not change significantly at low magnification. At high magnification, however, some of the nuclei in the spiral ganglion region are knotted and stained deeper, and the whole cell is spindle-shaped. Immunofluorescence staining of neurofilaments showed that the protein fluorescence intensity in the apex, middle, and base SGN and the central axis of the cochlea in the p10d group was significantly lower than that in the control group (Figure 7). These data suggest that RISNHL may be related to SGN morphological changes and neural conduction function.

 doi:10.20944/preprints202401.1522.v1

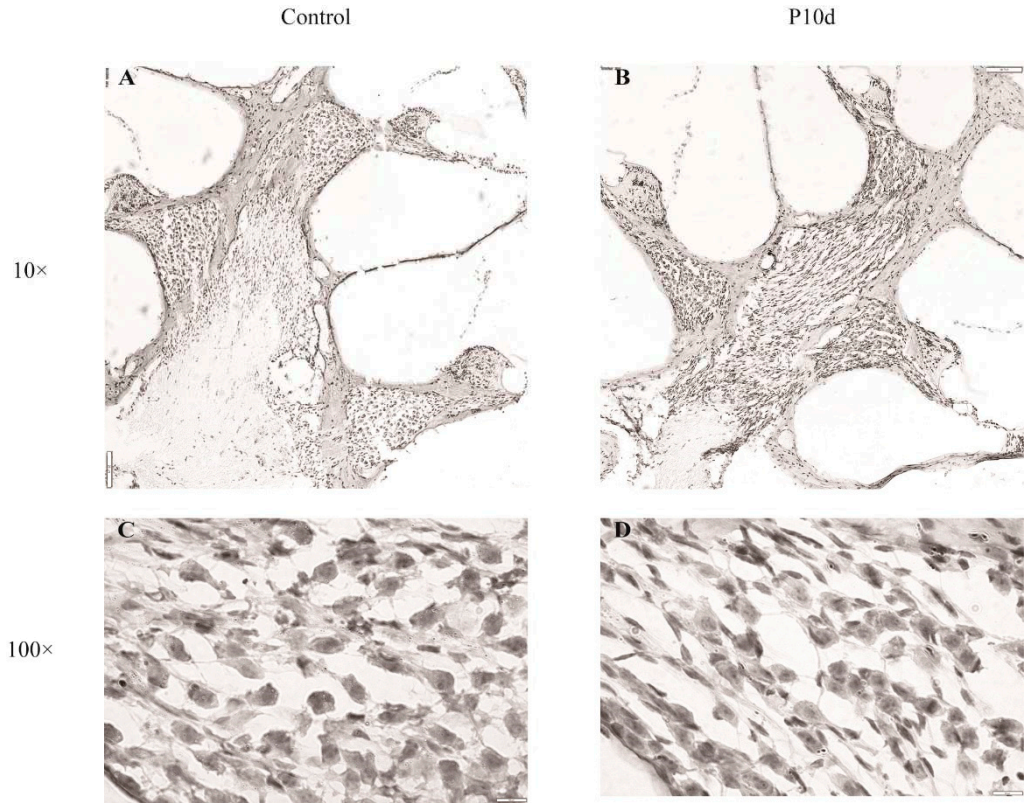

Figure 6. HE staining of cochlear slices. (**a**) Cochlear of the control group under 10x objective view. (**b**) Cochlear from the P10d group under an objective view of 10x. (**c**) Cochlear spiral ganglion cells of the control group under an objective view of 100x. (**d**) Cochlear spiral ganglion cells of the P10d group under 100x objective view.

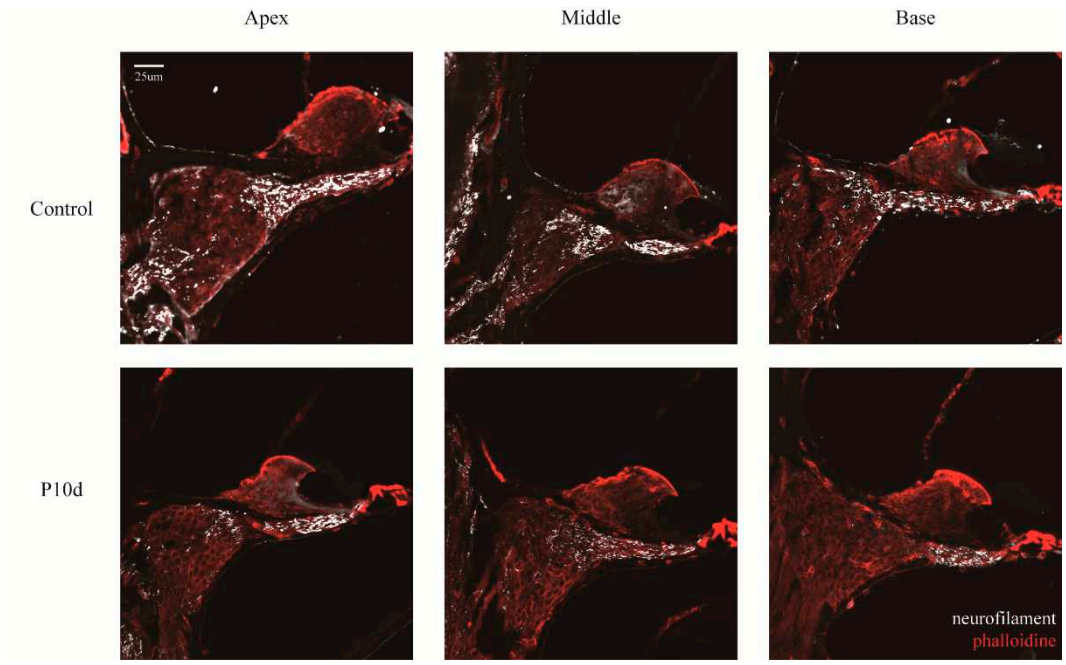

Figure 7. Cochlear neurofilament immunofluorescence staining. Immunofluorescence labeling of neurofilament protein in cochlear spiral ganglion region of the control group and P10d group at 40 × magnification. White: neurofilament; Red: phalloidin.

4. Discussion

The high dose of irradiation caused a dramatic reduction of macrophages in the inner ear. Traditionally, the inner ear has been wrongly recognized as an "immune privileged" organ due to the blood-labyrinth barrier. Our previous studies have confirmed that macrophages exist in stria vascularis, basilar membrane, and SGN, and perivascular resident macrophages in the stria vascularis are essential for the integrity of the blood-labyrinth barrier and cochlear internal environment [21]. Cochlear macrophages are the primary immune cells in the cochlea and play an important role in maintaining homeostasis in the immune microenvironment of the inner ear. The migration and activity of macrophages show complicated changes after cochlear injury, including noise [14], toxins, ototoxic antibiotics, or viral infection. Regulation of macrophage-mediated immune response may be a therapeutic approach to various trauma-induced hearing loss [15,21,22]. Macrophages have been found to increase and aggregate in the sensory epithelial damaged area both in the noise-induced hearing loss [23] model and connexin26 deficiency hearing loss model [15]. However, we first find that cochlear macrophages are significantly reduced in our radiation-induced hearing loss model. This result is consistent with some previous in-vitro studies, which have reported little in animal models of local radiation. The proliferation of bone marrow-derived macrophages can be almost complete inhibition within 72 hours after 10 Gy γ-radiation through direct DNA damage and caspase-1-mediated pyroptosis mechanism [24]. Researchers also suggested that ionizing radiation promotes macrophage polarization patterns toward a proinflammatory M1-like phenotype [25,26]. Our experiment also observed radiation caused bone marrow suppression [27] in mice, which is characterized by the rapid decrease of white blood cells, platelets, lymphocytes, and intermediate cells in circulation. Therefore, we speculate that high-dose irradiation not only kills the cochlea macrophages but also blocks the chemotactic recruitment of circulating macrophages to the inner ear. Radiation-induced activation of macrophages produces damaging bystander signals [24,26]. It is known that M1 macrophages can secrete cytotoxic pro-inflammatory factors such as IL-1, IL-6, IL-12, and TNF-α. M2 macrophages promote to repair the damaged tissue through the expression of anti-inflammatory factors, including Arginase-1, CD206, and IL-4RA [28]. Low-dose irradiation generally promotes macrophage polarization toward the anti-inflammatory M2 phenotype, while high-dose irradiation is more likely to augment the pro-inflammatory properties of macrophages and promote the expression of various pro-inflammatory genes (IL-1β, IL-6, CCL2, and TNF-α) [26,29]. In vivo, irradiation enhanced the M1-like features of macrophages from CBA/Caj mice [30]. Cranial radiotherapy-mediated bystander effect, neuroinflammation, and immune cell infiltration are dependent on macrophage-associated immune response [31]. Our experiment shows that high-dose radiation of CBA/Caj mice cranial led to immune microenvironment disturbance of the inner ear, as shown by rapid up-regulation of inner ear IL-1β, IL-6, TNF-α, and CCL2 on the first day after radiation. As the number of macrophages decreases, the expression of inflammatory factors also decreases in a time-dependent manner. We speculate here that the bystander effect induced by high doses of irradiation, including changes in SGN cell and neurofilament expression, may be mediated by activation of the M1-like proinflammatory response.

Ionizing radiation not only suppresses tumor cells but also causes radioactive damage to normal tissue. The causes of bystander cell damage are as follows: On the one hand, ionizing radiation can directly cause DNA damage and cell death. On the other hand, radiation can indirectly promote cell-cycle arrest, cell senescence, necrosis, or apoptosis through excessive oxidative stress and inflammation [12,32], which eventually leads to tissue microenvironment destruction and functional disorder [33]. During the treatment of head and neck cancer, sensorineural hearing loss is one of the "radiation-induced bystander effects". Ionizing radiation can indirectly damage auditory-associated cells and structures, resulting in auditory abnormalities and vestibular dysfunction. Previous studies have observed changes in inner ear structure and auditory function in the chronic phase after exposure to low to moderate-intensity radiation. Earlier in the 1970s, G M Thibadoux et al. serially assessed the hearing sensitivity of 61 children treated with 2,400 rads of cranial radiation, and the assessments of individual audiograms revealed that none of the children had any significant reductions in hearing levels at 3 years after exposure [34]. Therefore, we speculate that low-dose radiation exposure has no significant effect on hearing. Pathological studies of the temporal bones of

nuclear power plant workers exposed to 20 hours of high-dose radiation revealed mild degeneration of cochlear SGN cells and sensory hair cells after 7 months [35]. D L Hoistad et al [36] studied histopathologic slides of human temporal bones after a total of 60-70Gy doses of radiotherapy. Loss of inner and outer hair cells, reduction of SGN cells, and atrophy of stria vascularis were demonstrated in groups receiving cis-platinum, radiation, and combination compared to normal controls. As a result, high-dose radiation can contribute to otologic sequelae including SNHL, vascular changes, serous effusion, or fibrosis. Keilty, Dana, et al. put forward that the cumulative incidence of HL was 50% or greater at 5 years after RT if the mean cochlea dose was > 30 Gy. A mean cochlea dose of ≤ 30 Gy is suggested as a goal to reduce the risk of HL [5]. In our model, there is no significant loss of basal membrane hair cells in mice after 30Gy X-ray exposure and no change in the ABR threshold during the first-week post-radiation. In the P10d group, the ABR threshold increases significantly for all tested frequencies, accompanied by a prolonged delay and a down-regulated amplitude of the ABR I wave. These results are at odds with many previous studies [3,5,17,37,38] that have highlighted the loss of outer hair cells in mice after irradiation. They also proposed that the hair cell loss at the basilar membrane is significantly higher than at the apex. Correspondingly, hearing loss occurs preferentially in the high-frequency region and then slowly moves toward the low-frequency region. Cell cycle regulation is the most important determinant of ionizing radiation sensitivity, with cells being most radiosensitive in the G (2) -M phase. Sometimes, radiation-induced DNA damage initiates signals that can ultimately activate irreversible growth arrest that results in cell death (necrosis or apoptosis) [39]. Cells with active proliferation and division (such as malignant tumor cell, stem cell) are mostly in the M phase of cell cycle, so they are very sensitive to radiation, which is the molecular biological principle of radiation therapy. On the contrary, terminally differentiated cells have lost the ability to divide so they are not sensitive to radiation, such as neuron, myocyte [40]. Therefore, sensory hair cells of the mammalian inner ear, as highly differentiated mature cells, cannot divide [41], so they are not sensitive to radiation. In our experiments, high-dose irradiation did not cause cochlear hair cell loss, in agreement with the above theory. Chronic hair cell loss caused by low/moderate-dose irradiation in some studies may be a manifestation of the "bystander effect". For example, Pyun, J. H. et al. [42] confirmed that 20Gy-photon beams induced ABR threshold shift in rat and auditory neuromast loss in the zebrafish. They also found apoptosis and intracellular ROS production in cortico-derived cell lines. Further experiments have shown that blocking ROS production may protect auditory cells from radiation in vitro and in vivo. Similarly, severe damage to the cochlea and vestibule induced by radiation was alleviated by an anti-inflammatory drug, which was confirmed to down-regulate the expression of pro-inflammatory factor TNF$\alpha$and upregulate the expression of anti-inflammatory factor IL-2 in the cochlea after radiation [43]. Our study is limited to results obtained within 10 days after a single 30Gy X-ray cranial irradiation of 8-week-old CBA/caj mice. At the same time, the health of the mice deteriorated after high doses of irradiation. Some P10d individuals were too weak to tolerate anesthesia, at which point the ABR audiometry may not reflect the true function of the mouse's cochlea.

Our results suggest that acute RISNHL is not caused by cochlear hair cell death, but may be related to the morphological changes of cochlear SGN and nerve conduction disorders [44]. These results are in agreement with a small number of previous studies. The study by Gasser Rutledge, K. L administered 10-60 Gy γ-ray radiation doses to the cranial of mice. They found significant ABR threshold shift occurred at all test frequencies in mice exposed to ≥ 20 Gy by 8 days post-irradiation, and the initial impact of radiation in the first-week post-exposure focuses on SGN cell bodies and peripheral projections. Neuronal density and extracellular matrix are dramatically reduced in the Rosenthal canal and spiral lamina. No differences were noted within the Gy group in the frequency or severity of pathology along the length of the cochlea. At the same time, hair cells, stria vascularis, and vasculature showed negligible changes [45]. Liu, Z., et al. [11] gave cobalt-60 rays at doses of 10 Gy or 20 Gy to mice heads, and they also verified no significant changes in the number of hair cells or the array for the treatments. The number and size of the pre-synaptic ribbons (labeled by anti-RIBEYE/CtBP2 antibody) and the expression of VGLUT-3 were downregulated by radiation, resulting in RISNHL. The acute RISNHL in our model may be induced by a potential impairment of

 doi:10.20944/preprints202401.1522.v1

the auditory conduction pathway after cranial irradiation. Studies have confirmed that ionizing radiation can directly damage nerve myelin, Schwann cells, and fibrin in short time [46], leading to nerve microfilaments and microtubules aggregation, nerve fiber density reduction, nerve inner and outer membrane fibrosis, nerve axons and myelin degeneration or even necrosis[47–49]. In our experiments, we hypothesize that SNHL in the short term of high-dose radiation may be associated with morphological changes in inner ear SGN cells and reduced neurofilament. Compared with the control group, the nuclei of the SGN were knotted and darker in color, and the whole cell was spindle-shaped in the mice exposed to the radiation. Atrophied cells have fewer organelles, especially the mitochondrial, leading to their ability to metabolize substances and respond to neuroendocrine stimuli downfall, and those atrophied cells will eventually die [50]. In the traumatic brain injury model, the loss of brain parenchyma was secondary to progressively neuronal atrophy and eventually programmed cell death [51]. Neurofilaments provide structural support to the highly asymmetric geometry of neurons and are essential for efficient neural conduction velocity. Neurofilaments in axons extensively interconnect with cytoskeletal elements, creating a regionally specialized network for material transport. Neurofilament subunits are also present in postsynaptic terminal buttons and may be involved in neurotransmission [44]. In our study, the atrophy of SGN cells and the down-regulation of neurofilament expression induced by high-dose irradiation are likely to be the main histopathological causes of hearing loss. Radiotherapy can cause auditory neuropathy and Schwann cell death leading to impaired hearing function [46]. Demyelination of the cochlea SGN (a precursor of neurodegeneration) is associated with impaired auditory neural synchrony [22]. Therefore, based on the above results, high doses of cranial irradiation may also cause other types of impairments in the auditory nervous system, which needs to be investigated further.

We find that localized irradiation leads to inhibition of cochlear and systemic immune cells, but is accompanied by increased levels of local tissue inflammation. In addition to the explanation of the M1-like proinflammatory response induced by high-dose irradiation, the underlying mechanism of this phenomenon needs to be further explored. In addition, we consider morphological changes in nerve cells and nerve fibers in the inner ear of P10d mice as a possible indication of neurodegeneration or even SGN cell death. These could explain the lack of hair cell loss in RISNHL. After exposure to high doses of ionizing radiation, the number of basilar macrophages decreases in a time-dependent manner and the inflammatory mediators in the cochlea transiently increase. In the future, if we increase the penetration of circulating macrophages into the cochlea or stimulate M2 phenotypic polarization in the inner ear, can we attenuate radiation toxicity and become therapeutic targets for RISNHL prevention? Also, the relationship between spiral ganglion cells, nerve filaments, inner ear neural pathways, inner ear macrophages, and changes in inflammation levels and auditory function needs to be further explored. If we use a neuroprotective agent, is it beneficial to slow down the development of RIHNSL? Moreover, cochlear veins are important for the maintenance of inner ear lymphatic circulation and electrophysiological function [52], but vascular endothelial cells are very sensitive to ionizing radiation [53]. A recent study confirmed that radiation causes the cochlear stria vascularis to become less tightly connected. The damage of the blood-labyrinthine barrier and the enhancement of vascular permeability in turn increases the accumulation of cochlear ROS [54] and eventually leads to RISNHL with significant loss of hair cells [9]. In addition, perivascular resident macrophage-like melanocytes from the stria vascularis of mice are a crucial component in maintaining the integrity and function of the blood-labyrinth barrier. Thus, the role of the oxidative stress mechanism in the overwhelming M1-like proinflammatory response induced by high doses of radiation in our RISNHL model remains unknown. Whether radiation damages perivascular resident macrophage-like melanocytes in the stria vascularis and whether it causes perturbations in the microcirculation of the inner ear requires further exploration. Acute inner ear inflammation induced by injection of LPS into the tympanum of the middle ear is caused by targeted infiltration and activation of immune cells [55]. The expression of proinflammatory factors in the pathological cochlea is increased, and the permeability of the blood-labyrinth barrier is enhanced, thus making it more sensitive to external toxic substances [56]. The acute phase of hearing loss due to bacterial meningitis is partially reversible, and permanent hearing loss due to meningitis after 2 weeks is caused by

 doi:10.20944/preprints202401.1522.v1

disruption of the blood labyrinth barrier and SGN necrosis (not apoptosis) [57]. We hypothesize that early regulation of cochlear immune cell infiltration may preserve hearing loss in acute deafness models.

Overall, this study is a suitable model for acute RISNHL, but observations of immune inflammation in the inner ear are limited due to radiation suppression of the immune system. The next step is to study the role of macrophage-related inflammatory response in regulating the auditory pathway (from sensorial epithelium to auditory cortex).

5. Conclusions

SNHL induced by high doses of radiation does not involve hair cell loss, but rather morphological changes in SGN cells. Short-term RISNHL is accompanied by a significant reduction in cochlear macrophages and variation in the immunological microenvironment. The underlying mechanisms between these results remain to be explored.

Author Contributions: Conceptualization and supervision, Y.S.; methodology, J.T. and C.L.; formal analysis, M.S. and J.T.; investigation, M.S., H.Y., and Y.W.; writing—original draft, M.S.; writing—review and editing, Y.S. and J.T.; All authors have read and agreed to the published version of the manuscript.

Funding: This research was funded by the Innovative Research Groups of Hubei Province (No. 2023AFA038), the National Natural Science Foundation of China (No. 82071058), the Fundamental Research Funds for the Central Universities (Grant No. YCJJ20230111), and the National Key Research and Development Program of China (No. 2021YFF0702303).

Institutional Review Board Statement: All animal procedures were performed in compliance with experimental guidelines approved by the Union Hospital of Tongji Medical College, Huazhong University of Science and Technology. Written informed consent was obtained from the owners for the participation of their animals in this study.

Informed Consent Statement: All experimental procedures were conducted in accordance with the policies of the Committee on Animal Research of Tongji Medical College, Huazhong University of Science and Technology (Permit No. 534).

Data Availability Statement: The datasets used and/or analyzed during the current study are available from the corresponding author on reasonable request.

Acknowledgments: We particularly thank KunYu Yang for his advice and suggestions on the radiation method. We grateful to Cancer center (Wuhan Union Hospital) for their help guidance and assistance with the radiation.

Conflicts of Interest: The authors declare no conflict of interest.

Ethic Committee Name: Committee on Animal Research of Tongji Medical College, Huazhong University of Science and Technology

> Approval Code: S1170

> Approval Date: 2019.03.05

References

1. Wang, X.; Hu, C.; Eisbruch, A., Organ-sparing radiation therapy for head and neck cancer. *Nat. Rev. Clin. Oncol.* **2011**, 8 (11), 639-648.
2. Lambert, E. M.; Gunn, G. B.; Gidley, P. W., Effects of radiation on the temporal bone in patients with head and neck cancer. *Head Neck* **2016**, 38 (9), 1428-1435.
3. Mujica-Mota, M. A.; Lehnert, S.; Devic, S.; Gasbarrino, K.; Daniel, S. J., Mechanisms of radiation-induced sensorineural hearing loss and radioprotection. *Hearing Research* **2014**, 312, 60-68.
4. Nichols, A. C.; Theurer, J.; Prisman, E.; Read, N.; Berthelet, E.; Tran, E.; Fung, K.; de Almeida, J. R.; Bayley, A.; Goldstein, D. P.; Hier, M.; Sultanem, K.; Richardson, K.; Mlynarek, A.; Krishnan, S.; Le, H.; Yoo, J.; MacNeil, S. D.; Winquist, E.; Hammond, J. A.; Venkatesan, V.; Kuruvilla, S.; Warner, A.; Mitchell, S.; Chen, J.; Corsten, M.; Johnson-Obaseki, S.; Eapen, L.; Odell, M.; Parker, C.; Wehrli, B.; Kwan, K.; Palma, D. A.,

Radiotherapy versus transoral robotic surgery and neck dissection for oropharyngeal squamous cell carcinoma (ORATOR): an open-label, phase 2, randomised trial. *Lancet Oncol.* **2019**, 20 (10), 1349-1359.

5. Keilty, D.; Khandwala, M.; Liu, Z. A.; Papaioannou, V.; Bouffet, E.; Hodgson, D.; Yee, R.; Cushing, S.; Laperriere, N.; Ahmed, S.; Mabbott, D.; Ramaswamy, V.; Tabori, U.; Huang, A.; Bartels, U.; Tsang, D. S., Hearing Loss After Radiation and Chemotherapy for CNS and Head-and-Neck Tumors in Children. *J. Clin. Oncol.* **2021**, 39 (34), 3813-3821.
6. Huang, Z.; Wang, Y.; Yao, D.; Wu, J.; Hu, Y.; Yuan, A., Nanoscale coordination polymers induce immunogenic cell death by amplifying radiation therapy mediated oxidative stress. *Nat. Commun.* **2021**, 12 (1), 145.
7. Bouchet, A.; Potez, M.; Coquery, N.; Rome, C.; Lemasson, B.; Bräuer-Krisch, E.; Rémy, C.; Laissue, J.; Barbier, E. L.; Djonov, V.; Serduc, R., Permeability of Brain Tumor Vessels Induced by Uniform or Spatially Microfractionated Synchrotron Radiation Therapies. International Journal of Radiation Oncology, Biology, Physics **2017**, 98 (5), 1174-1182.
8. Gu, J.; Tong, L.; Lin, X.; Chen, Y.; Wu, H.; Wang, X.; Yu, D., The disruption and hyperpermeability of blood-labyrinth barrier mediates cisplatin-induced ototoxicity. *Toxicol. Lett.* 2022, 354, 56-64.
9. Yiming, G.; Fan, W.; Wuhui, H.; Ziyi, C.; Jiaqi, P.; Yiqing, Z., ROS-related disruptions to cochlear hair cell and stria vascularis consequently leading to radiation-induced sensorineural hearing loss. *Antioxid. Redox. Signal.* **2023**.
10. Jiang, H.-Y.; Yang, Y.; Zhang, Y.-Y.; Xie, Z.; Zhao, X.-Y.; Sun, Y.; Kong, W.-J., The dual role of poly (ADP-ribose) polymerase-1 in modulating parthanatos and autophagy under oxidative stress in rat cochlear marginal cells of the stria vascularis. *Redox Biol.* **2018**, 14, 361-370.
11. Liu, Z.; Luo, Y.; Guo, R.; Yang, B.; Shi, L.; Sun, J.; Guo, W.; Gong, S.; Jiang, X.; Liu, K., Head and neck radiotherapy causes significant disruptions of cochlear ribbon synapses and consequent sensorineural hearing loss. *Radiother. Oncol.* **2022**, 173, 207-214.
12. Barrett, C.; Hellickson, I.; Ben-Avi, L.; Lamb, D.; Krahenbuhl, M.; Cerveny, K. L., Impact of Low-level Ionizing Radiation on Cell Death During Zebrafish Embryonic Development. *Health Phys.* **2018**, 114 (4), 421-428.
13. Zuo, W.-Q.; Hu, Y.-J.; Yang, Y.; Zhao, X.-Y.; Zhang, Y.-Y.; Kong, W.; Kong, W.-J., Sensitivity of spiral ganglion neurons to damage caused by mobile phone electromagnetic radiation will increase in lipopolysaccharide-induced inflammation in vitro model. *J. Neuroinflammation.* **2015**, 12, 105.
14. Manickam, V.; Gawande, D. Y.; Stothert, A. R.; Clayman, A. C.; Batalkina, L.; Warchol, M. E.; Ohlemiller, K. K.; Kaur, T., Macrophages Promote Repair of Inner Hair Cell Ribbon Synapses following Noise-Induced Cochlear Synaptopathy. *J. Neurosci.* **2023**, 43 (12), 2075-2089.
15. Xu, K.; Chen, S.; Xie, L.; Qiu, Y.; Bai, X.; Liu, X. Z.; Zhang, H. M.; Wang, X. H.; Jin, Y.; Sun, Y.; Kong, W. J., Local Macrophage-Related Immune Response Is Involved in Cochlear Epithelial Damage in Distinct Gjb2-Related Hereditary Deafness Models. *Front. Cell Dev. Biol.* **2020**, 8, 597769.
16. Murray, P. J.; Wynn, T. A., Protective and pathogenic functions of macrophage subsets. *Nat. Rev. Immunol.* **2011**, 11 (11), 723-737.
17. Liu, J.; Zhu, L.; Bao, Y.; Du, Z.; Shi, L.; Hong, X.; Zou, Z.; Peng, G., Injectable dexamethasone-loaded peptide hydrogel for therapy of radiation-induced ototoxicity by regulating the mTOR signaling pathway. *J. Control. Release* **2023**, 365, 729-743.
18. Polonenko, M. J.; Maddox, R. K., Optimizing Parameters for Using the Parallel Auditory Brainstem Response to Quickly Estimate Hearing Thresholds. *Ear Hear.* **2022**, 43 (2), 646-658.
19. Gibbs, A.; Gupta, P.; Mali, B.; Poirier, Y.; Gopalakrishnan, M.; Newman, D.; Zodda, A.; Down, J. D.; Serebrenik, A. A.; Kaytor, M. D.; Jacksone, I. L., A C57L/J Mouse Model of the Delayed Effects of Acute Radiation Exposure in the Context of Evolving Multi-Organ Dysfunction and Failure after Total-Body Irradiation with 2.5% Bone Marrow Sparing. *Radiat. Res.* **2023**, 199 (4), 319-335.
20. Wu, S.-Y.; Hsieh, C.-C.; Wu, R.-R.; Susanto, J.; Liu, T.-T.; Shen, C.-R.; Chen, Y.; Su, C.-C.; Chang, F.-P.; Chang, H.-M.; Tosh, D.; Shen, C.-N., Differentiation of pancreatic acinar cells to hepatocytes requires an intermediate cell type. *Gastroenterology* **2010**, 138 (7), 2519-2530.
21. He, W.; Yu, J.; Sun, Y.; Kong, W., Macrophages in Noise-Exposed Cochlea: Changes, Regulation and the Potential Role. *Aging Dis.* 2020, 11 (1), 191-199.

22. Pan, H.; Song, Q.; Huang, Y.; Wang, J.; Chai, R.; Yin, S.; Wang, J., Auditory Neuropathy after Damage to Cochlear Spiral Ganglion Neurons in Mice Resulting from Conditional Expression of Diphtheria Toxin Receptors. *Sci. Rep.* **2017**, 7 (1), 6409.
23. Mizushima, Y.; Fujimoto, C.; Kashio, A.; Kondo, K.; Yamasoba, T., Macrophage recruitment, but not interleukin 1 beta activation, enhances noise-induced hearing damage. *Biochem. Biophys. Res. Commun.* **2017**, 493 (2), 894-900.
24. Hu, B.; Jin, C.; Li, H.-B.; Tong, J.; Ouyang, X.; Cetinbas, N. M.; Zhu, S.; Strowig, T.; Lam, F. C.; Zhao, C.; Henao-Mejia, J.; Yilmaz, O.; Fitzgerald, K. A.; Eisenbarth, S. C.; Elinav, E.; Flavell, R. A., The DNA-sensing AIM2 inflammasome controls radiation-induced cell death and tissue injury. *Science* **2016**, 354 (6313), 765-768.
25. Tabraue, C.; Lara, P. C.; De Mirecki-Garrido, M.; De La Rosa, J. V.; Lopez-Blanco, F.; Fernandez-Perez, L.; Bosca, L.; Castrillo, A., LXR Signaling Regulates Macrophage Survival and Inflammation in Response to Ionizing Radiation. *Int. J. Radiat. Oncol. Biol. Phys.* **2019**, 104 (4), 913-923.
26. Kang, H.; Kim, S.-C.; Oh, Y., Fucoxanthin Abrogates Ionizing Radiation-Induced Inflammatory Responses by Modulating Sirtuin 1 in Macrophages. *Mar. Drugs* **2023**, 21 (12).
27. Zhang, X.; Hou, L.; Li, F.; Zhang, W.; Wu, C.; Xiang, L.; Li, J.; Zhou, L.; Wang, X.; Xiang, Y.; Xiao, Y.; Li, S. C.; Chen, L.; Ran, Q.; Li, Z., Piezo1-mediated mechanosensation in bone marrow macrophages promotes vascular niche regeneration after irradiation injury. *Theranostics* **2022**, 12 (4), 1621-1638.
28. Blériot, C.; Chakarov, S.; Ginhoux, F., Determinants of Resident Tissue Macrophage Identity and Function. *Immunity* **2020**, 52 (6), 957-970.
29. Wu, Q.; Allouch, A.; Martins, I.; Modjtahedi, N.; Deutsch, E.; Perfettini, J. L., Macrophage biology plays a central role during ionizing radiation-elicited tumor response. *Biomed. J.* **2017**, 40 (4), 200-211.
30. Rastogi, S.; Boylan, M.; Wright, E. G.; Coates, P. J., Interactions of apoptotic cells with macrophages in radiation-induced bystander signaling. *Radiat. Res.* **2013**, 179 (2), 135-145.
31. Moravan, M. J.; Olschowka, J. A.; Williams, J. P.; O'Banion, M. K., Brain radiation injury leads to a dose- and time-dependent recruitment of peripheral myeloid cells that depends on CCR2 signaling. *J. Neuroinflammation* **2016**, 13, 30.
32. Hu, L.; Yin, X.; Zhang, Y.; Pang, A.; Xie, X.; Yang, S.; Zhu, C.; Li, Y.; Zhang, B.; Huang, Y.; Tian, Y.; Wang, M.; Cao, W.; Chen, S.; Zheng, Y.; Ma, S.; Dong, F.; Hao, S.; Feng, S.; Ru, Y.; Cheng, H.; Jiang, E.; Cheng, T., Radiation-induced bystander effects impair transplanted human hematopoietic stem cells via oxidative DNA damage. *Blood* **2021**, 137 (24), 3339-3350.
33. Mittra, I.; Samant, U.; Sharma, S.; Raghuram, G. V.; Saha, T.; Tidke, P.; Pancholi, N.; Gupta, D.; Prasannan, P.; Gaikwad, A.; Gardi, N.; Chaubal, R.; Upadhyay, P.; Pal, K.; Rane, B.; Shaikh, A.; Salunkhe, S.; Dutt, S.; Mishra, P. K.; Khare, N. K.; Nair, N. K.; Dutt, A., Cell-free chromatin from dying cancer cells integrate into genomes of bystander healthy cells to induce DNA damage and inflammation. *Cell Death Discov.* **2017**, 3, 17015.
34. Thibadoux, G. M.; Pereira, W. V.; Hodges, J. M.; Aur, R. J., Effects of cranial radiation on hearing in children with acute lymphocytic leukemia. *J. Pediatr.* **1980**, 96 (3 Pt 1), 403-406.
35. Kaga, K.; Maeshima, A.; Tsuzuku, T.; Kondo, K.; Morizono, T., Temporal bone histopathological features of a worker who received high doses of radiation in a criticality accident: a case report. *Acta Otolaryngol.* **2011**, 131 (4), 451-455.
36. Hoistad, D. L.; Ondrey, F. G.; Mutlu, C.; Schachern, P. A.; Paparella, M. M.; Adams, G. L., Histopathology of human temporal bone after cis-platinum, radiation, or both. *Otolaryngol. Head Neck Surg.* **1998**, 118 (6), 825-832.
37. Yang, C.; Zhang, W.; Liu, X.-L.; Liang, Y.; Yuan, Y.-W.; Ren, C.; Peng, J.-H., Localization of prestin and expression in the early period after radiation in mice. *Eur. Arch. Otorhinolaryngol.* **2014**, 271 (12), 3333-3340.
38. Giese, A. P. J.; Guarnaschelli, J. G.; Ward, J. A.; Choo, D. I.; Riazuddin, S.; Ahmed, Z. M., Radioprotective Effect of Aminothiol PrC-210 on Irradiated Inner Ear of Guinea Pig. *PLoS One* **2015**, 10 (11), e0143606.
39. Pawlik, T. M.; Keyomarsi, K., Role of cell cycle in mediating sensitivity to radiotherapy. *Int. J. Radiat. Oncol. Biol. Phys.* **2004**, 59 (4), 928-942.
40. Coffman, J. A., Cell cycle development. *Dev. Cell* **2004**, 6 (3), 321-327.
41. Edge, A. S.; Chen, Z.-Y., Hair cell regeneration. *Curr. Opin. Neurobiol.* **2008**, 18 (4), 377-382.

42. Pyun, J. H.; Kang, S. U.; Hwang, H. S.; Oh, Y. T.; Kang, S. H.; Lim, Y. A.; Choo, O. S.; Kim, C. H., Epicatechin inhibits radiation-induced auditory cell death by suppression of reactive oxygen species generation. *Neuroscience* **2011**, 199, 410-420.
43. Zhang, J.; Xu, A.; Niu, T.; Liu, C.; Zhang, Y.; Li, T.; Wang, J.; Wang, Y.; Sun, D., A unique radioprotective effect of resolvin E1 reduces irradiation-induced damage to the inner ear by inhibiting the inflammatory response. Radiat Oncol **2020**, 15 (1), 223.
44. Yuan, A.; Rao, M. V.; Veeranna; Nixon, R. A., Neurofilaments and Neurofilament Proteins in Health and Disease. *Cold Spring Harb. Perspect. Biol.* **2017**, 9 (4).
45. Gasser Rutledge, K. L.; Prasad, K. G.; Emery, K. R.; Mikulec, A. A.; Varvares, M.; Gratton, M. A., Short-term Peripheral Auditory Effects of Cranial Irradiation: A Mouse Model. *Ann. Otol. Rhinol. Laryngol.* **2015**, 124 (11), 903-10.
46. Dinh, C. T.; Chen, S.; Nourbakhsh, A.; Padgett, K.; Johnson, P.; Goncalves, S.; Bracho, O.; Bas, E.; Bohorquez, J.; Monje, P. V.; Fernandez-Valle, C.; Elsayyad, N.; Liu, X.; Welford, S. M.; Telischi, F., Single Fraction and Hypofractionated Radiation Cause Cochlear Damage, Hearing Loss, and Reduced Viability of Merlin-Deficient Schwann Cells. *Cancers (Basel)* **2023**, 15 (10).
47. Irvine, K. A.; Blakemore, W. F., Remyelination protects axons from demyelination-associated axon degeneration. *Brain* **2008**, 131 (Pt 6), 1464-1477.
48. Lee, R. X.; Tang, F. R., Radiation-induced neuropathological changes in the oligodendrocyte lineage with relevant clinical manifestations and therapeutic strategies. *Int. J. Radiat. Biol.* **2022**, 98 (10), 1519-1531.
49. Masurovsky, E. B.; Bunge, M. B.; Bunge, R. P., Cytological studies of organotypic cultures of rat dorsal root ganglia following X-irradiation in vitro. II. Changes in Schwann cells, myelin sheaths, and nerve fibers. *J. Cell Biol.* 1967, 32 (2), 497-518.
50. Schwartz, L. M., Atrophy and programmed cell death of skeletal muscle. *Cell Death Differ.* **2008**, 15 (7), 1163-1169.
51. Ramirez, S.; Mukherjee, A.; Sepulveda, S.; Becerra-Calixto, A.; Bravo-Vasquez, N.; Gherardelli, C.; Chavez, M.; Soto, C., Modeling Traumatic Brain Injury in Human Cerebral Organoids. *Cells* **2021**, 10 (10).
52. Hirose, K.; Li, S.-Z., The role of monocytes and macrophages in the dynamic permeability of the blood-perilymph barrier. *Hear. Res.* **2019**, 374, 49-57.
53. Low, W.-K.; Tan, M. G. K.; Chua, A. W. C.; Sun, L.; Wang, D.-Y., 12th Yahya Cohen Memorial Lecture: The cellular and molecular basis of radiation-induced sensori-neural hearing loss. *Ann. Acad. Med. Singap.* **2009**, 38 (1), 91-94.
54. Zhang, Y.; Yang, Y.; Xie, Z.; Zuo, W.; Jiang, H.; Zhao, X.; Sun, Y.; Kong, W., Decreased Poly (ADP-Ribose) Polymerase 1 Expression Attenuates Glucose Oxidase-Induced Damage in Rat Cochlear Marginal Strial Cells. *Mol. Neurobiol.* **2016**, 53 (9), 5971-5984.
55. Bae, S. H.; Yoo, J. E.; Choe, Y. H.; Kwak, S. H.; Choi, J. Y.; Jung, J.; Hyun, Y.-M., Neutrophils infiltrate into the spiral ligament but not the stria vascularis in the cochlea during lipopolysaccharide-induced inflammation. *Theranostics* **2021**, 11 (6), 2522-2533.
56. Chai, Y.; He, W.; Yang, W.; Hetrick, A. P.; Gonzalez, J. G.; Sargsyan, L.; Wu, H.; Jung, T. T. K.; Li, H., Intratympanic Lipopolysaccharide Elevates Systemic Fluorescent Gentamicin Uptake in the Cochlea. *Laryngoscope* **2021**, 131 (9), E2573-E2582.
57. Klein, M.; Koedel, U.; Pfister, H.-W.; Kastenbauer, S., Morphological correlates of acute and permanent hearing loss during experimental pneumococcal meningitis. *Brain Pathol.* **2003**, 13 (2), 123-132.